Journal of Coastal Research	35	4	852–860	Coconut Creek, Florida	July 2019

A Tentative Record of Mid-Holocene Sea-Level Highstand and Barrier Overwash from the Cam River Mouth, Vietnam

Harry Williams[†]*, Long Van Hoang[‡], Patrick Elliott[†], Hiep Huu Nguyen[‡], and Ha Manh[‡]

[†]Department of Geography and the Environment
University of North Texas
Denton, TX 76203, U.S.A.

[‡]Hanoi University of Mining and Geology
Hanoi, Vietnam

www.cerf-jcr.org

www.JCRonline.org

ABSTRACT

Williams, H.; Van Hoang, L.; Elliott, P.; Nguyen, H.H., and Manh, H., 2019. A tentative record of mid-Holocene sea-level highstand and barrier overwash from the Cam River mouth, Vietnam. *Journal of Coastal Research,* 35(4), 852–860. Coconut Creek (Florida), ISSN 0749-0208.

A freshwater coastal marsh near the mouth of the Cam River in Northern Vietnam stands 2–3 m above mean sea level and is bordered by a coastal barrier that reaches about 6 m above mean sea level. A core from the marsh contains a 14-cm-thick sand and shell layer. The presence of abundant shell fragments suggests inland transport of littoral sediment, and the sand layer is tentatively identified as a washover deposit. The coast of the study area contains a beachrock standing above the modern beach and reaching to ~4 m above mean sea level. A tentative explanation of this beachrock is that it represents a beach that formed during a mid-Holocene 2–3-m highstand, evidence for which has been reported from Thailand, Malaysia, Singapore, and Vietnam. Possible explanations of the sand and shell layer include the following: it is a late-Holocene tropical cyclone washover deposit, formed by a large storm surge that overtopped the coastal barrier; or it is a late-Holocene tsunami deposit formed when a tsunami wave, probably from a nearby source, overtopped the coastal barrier. The lack of other distinctive washover deposits in the core suggests that overwash of a magnitude that formed the relatively thick sand and shell layer is a rare event at this site within the last 3000 years. Given the tentative but intriguing results of this study, further research at this site is warranted to better define the stratigraphy and age of the apparent washover deposit.

ADDITIONAL INDEX WORDS: *Paleotempestology, beachrock, overwash, washover, tsunami.*

INTRODUCTION

The coast of Vietnam, bordering the South China Sea in the south and the Gulf of Tonkin in the north, is subject to powerful typhoon strikes that cause great loss of life, devastation of agricultural crops, and massive infrastructure damage. Typhoons affecting Vietnam originate in the NW Pacific Ocean and move in a W or NW direction. Some typhoons strike the Vietnamese coast directly, traveling westward across the South China Sea or curving north through the Gulf of Tonkin; others cross Hainan Island to strike the north coast of Vietnam. Notable typhoons that caused devastation in the region and made landfall on the coast of Vietnam in recent decades include Typhoon Xangsane (2006, Category 4, 312 fatalities, $750 million in damages); Typhoon Durian (2006, Category 4, 98 fatalities, $530 million in damages); Typhoon Ketsana (2009, Category 2, 710 fatalities, $1.09 billion in damages); Typhoon Nesat (2011, Category 4, 98 fatalities, $2.12 billion in damages); Typhoon Son Tinh (2012, Category 3, 42 fatalities, $576 million in damages); and Typhoon Doksuri (2017, Category 3, 20 fatalities, $793 million in damages) (Figure 1).

These and other recent catastrophic typhoon strikes throughout Southeast Asia highlight the need for better understanding of typhoon risk and impacts. For example, questions have been raised about the role of anthropogenic climate change in driving future tropical cyclone hazards. The way in which tropical cyclone activity will change under ongoing global warming is consequently an area of strong societal concern and scientific interest. In response to this question, recent tropical cyclone climatology research has focused on linking evidence of millennial-scale tropical cyclone variability to climatic changes within the Holocene. The underlying premise of these studies is that changing climatic conditions, such as sea-surface temperatures or the position of high- and low-pressure centers, can change the location and frequency of tropical cyclogenesis, increase the intensity of tropical cyclones, or affect atmospheric steering mechanisms, preferentially guiding more tropical cyclones into a particular region. A major goal of these studies is to develop historical and prehistorical analogs for future climate scenarios (Bengtsson *et al*., 2007; Camargo, 2013; Christensen *et al*., 2013; Elsner and Liu, 2003; Emanuel, 2013; Emanuel and Nolan, 2004; Fan and Liu, 2008; Frappier *et al*., 2007; Gualdi, Scoccimarro, and Navarra, 2008; Knutson *et al*., 2010; McCloskey, Bianchette, and Liu, 2013; Murakami, Mizuta, and Shindo, 2012; Murakami, Wang, and Kitoh, 2011; Murakami *et al*., 2012; Nott and Hayne, 2001; Pielke *et al*., 2005; Stowasser, Wang, and Hamilton, 2007; Sugi, Yoshida, and Murakami, 2015; Tory *et al*., 2013; Walsh, 2014; Walsh *et al*., 2014; Webster *et al*., 2005; Ying *et al*., 2012).

Because catastrophic tropical cyclones are rare events, this research depends on the availability of long-term records of tropical cyclone strikes. Historical meteorological records are mostly of too limited a time span, even when extended by analysis of documentary evidence (García-Herrera *et al*., 2004, 2005, 2007; Grossman and Zaiki, 2009; Liu, Shen, and Louie,

DOI: 10.2112/JCOASTRES-D-18-00126.1 received 3 September 2018; accepted in revision 14 November 2018; corrected proofs received 19 December 2018.
*Corresponding author: HarryF.Williams@unt.edu

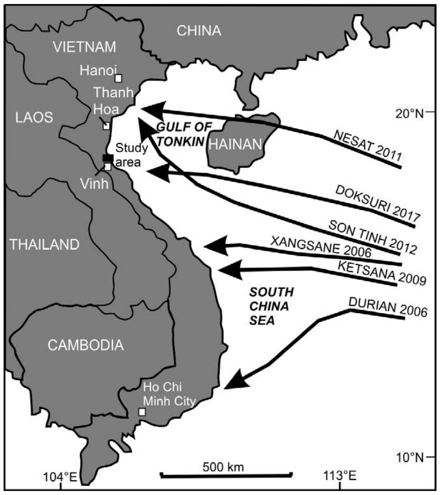

Figure 1. Location of study area between Vinh and Thanh Hoa on the Gulf of Tonkin coast. Tracks and approximate landfall locations of recent damaging typhoons are shown.

2001; Mock, 2004), and there are large gaps in geographic coverage of historical data occur. In response to the limitations of historical records, paleotempestological approaches have been developed that use geologic and biologic proxies of tropical cyclone strikes to construct much longer prehistorical records of tropical cyclone activity. A common approach is to use the sediment-based proxy of identifying and dating washover sand layers in aggrading lake, lagoon, pond, swamp, or marsh deposits located immediately landward of sandy barriers (Donnelly, 2005; Donnelly *et al.*, 2001a,b, 2004; Donnelly and Woodruff, 2007; Hodge and Williams, 2016; Lane *et al.*, 2011; Liu and Fearn, 1993, 2000a,b; McCloskey and Keller, 2009; Yu *et al.*, 2009). This approach has proven successful; for example, Williams *et al.* (2016) found geologic evidence of an 8000-year record of typhoon strikes on the coast of Thailand based on washover sand beds in coastal marshes and beach ridge plain swales. The typhoon record from Thailand supports the findings of other studies in the western North Pacific that suggest millennial-scale variability in typhoon frequency may be linked to Holocene climatic changes (Chan, 1985; Elsner and Liu, 2003; Liu, Shen, and Louie, 2001; Woodruff, Donnelly, and Okusu, 2009).

Relatively little research has been completed on typhoon washover sedimentation in Vietnam. Switzer *et al.* (2011) describe washover sand sheets attributed to Typhoon Xangsane (2006) and Typhoon Ketsana (2009), both of which made landfall in central Vietnam (Figure 1). In each case, the typhoon storm surge deposited scattered cobble to boulder-sized clasts within sand sheets that contrasted in sedimentary characteristics, reflecting differences in sediment sources and local depositional conditions. Currently, no published long-term records of prehistoric typhoon strikes on Vietnam exist. This paper reports results of a paleotempestological study aimed at identifying and dating geological evidence of prehistoric typhoon strikes preserved in coastal marshes on the Gulf of Tonkin coast in Northern Vietnam.

Study Area

The study area is located near the mouth of the River Cam and is one of several sites investigated between the cities of Vinh and Thanh Hoa, on the Gulf of Tonkin coast (Figure 1). This was the only site where rapid reconnaissance gouge coring indicated a substantial anomalous sand layer within the subsurface. The site is a large freshwater marsh, currently used for rice production. The marsh has developed between two bedrock headlands and is bordered on the seaward side by a wooded dune barrier, reaching up to about 6.4 m above mean sea level. The marsh surface is about 2–3 m above mean sea level and is presumably part of an extensive system of marine terraces in this part of Vietnam, formed by tidal flat, deltaic, and floodplain deposition during a mid-Holocene highstand of sea level (Nguyen, 1991; Pirazzoli, 1991; Tanabe, 2003; Tanabe *et al.*, 2006) (Figure 2).

Reconnaissance coring at this site, using a gouge corer, revealed tentative evidence for an extensive subsurface sand sheet. Gouge cores 1, 2, and 3, located 300–500 m into the marsh from the base of the dunes, contained no sand layers. Gouge cores 4 and 6, 250 m and 100 m from the base of the dunes, respectively, each contained a thin but distinct sand layer at depths of 40 cm and 25 cm, respectively. Both sand layers had a sharp lower contact with enclosing muddy marsh sediments. Gouge core 5, which is 175 m from the base of the dunes, did not contain any sand layers; gouge core 7, which is 30 m from the base of the dunes, contained a mixture of mud and sand throughout the core with no distinct sand layers (Figure 2).

METHODS

To follow up on the gouge core survey, a series of seven larger cores was obtained along a transect approximately perpendicular to the base of the dunes, extending from 30 to 400 m into the marsh (Figure 2). Core locations were recorded by a hand-held GPS with reported accuracy of ± 10 m (Garmin, 2007). The larger cores were collected from the marsh by driving thin-walled 7.5-cm-diameter aluminum tubes into the marsh deposits until coring was stopped by resistance.

A vacuum seal was placed in the top of the core tube to keep the sediment core in place, and the tubes were extracted from the marsh using a truck jack. Compaction occurred in all cores and was assessed by comparing the depth of penetration of the coring tube and the distance between the top of the sediment core inside the tube and the ground surface. This allowed compaction to be calculated as a percentage of core length. Uncompacted depths within cores were estimated by applying the compaction percentage uniformly over the entire length of the core. Cores were sealed and transported to a laboratory at the Hanoi University of Mining and Geology, where the tubes were cut lengthwise and the sediment cores within were split into two halves longitudinally.

Only core V3, located about 250 m from the base of the dunes, contained a recognizable sand layer at a (uncompacted) depth of 41–55 cm within the core (see Figure 2 for location of core V3). This core was sampled at 1-cm intervals for textural, loss-on-ignition, and microfossil analyses to examine contrasts in lithology and microfossil content between the sand layer and the enclosing marsh sediments.

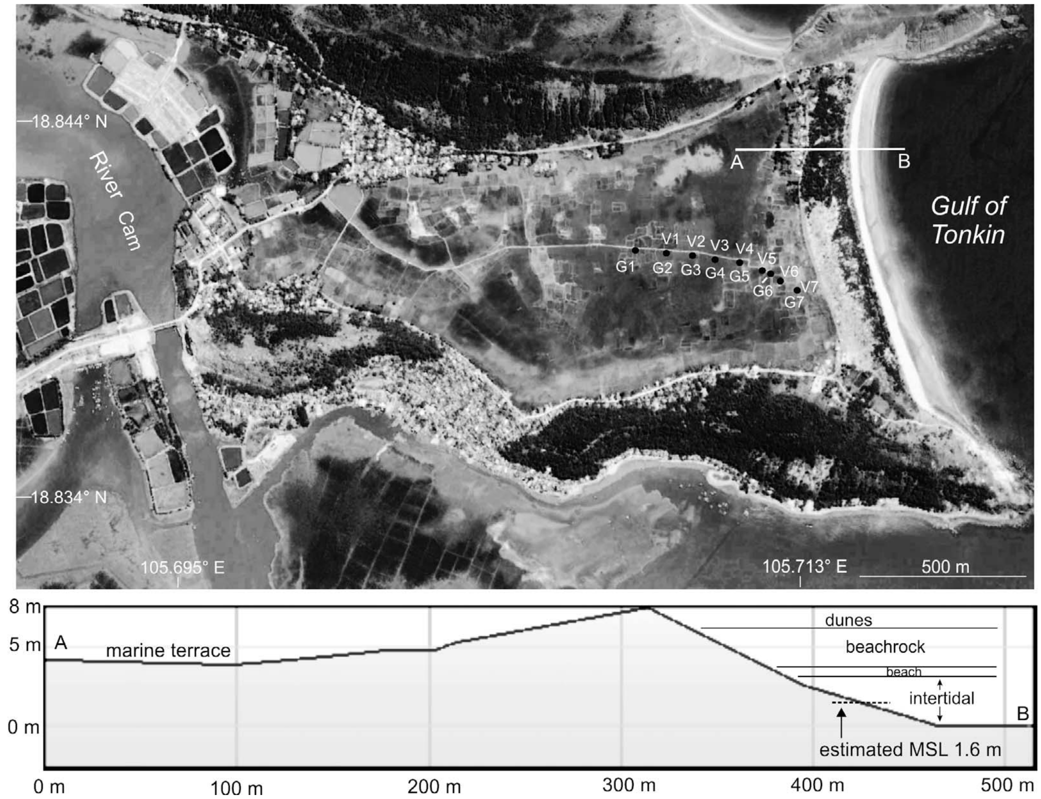

Figure 2. Location of cores (G: gouge core; V: larger-diameter core) and topographic profile A–B (Google Earth image, 2018).

All samples were divided into two subsamples for analysis. One subsample was weighed and then oven-dried at 105°C for 24 hours to determine moisture content (% wet weight). The other subsample was weighed and then wet-sieved through a 63-μm sieve to retain the sand fraction. The sand fraction was air-dried and weighed. The measured moisture content was used to calculate the dry weight of the sieved sample, and the weight of the sand fraction was then used to calculate sand content (% dry weight). The dried subsample was weighed and then placed in a muffle furnace at 550°C for 4 hours to determine organic matter content (% dry weight). After reweighing, the same sample was returned to the muffle furnace for 2 hours at 950°C to determine carbonate mineral content (% dry weight). The loss-on-ignition procedures follow the recommendation of Heiri, Lotter, and Lemcke (2001) for consistency; all samples had uniform treatment in terms of sample size, furnace temperatures, and furnace exposure times.

Sand fractions derived from wet sieving were examined under a dissecting microscope to identify and count foraminifers. If the sand fraction was small (<1 g), the entire sample was examined for foraminifers; if the sand fraction was large (>1 g), a dry splitter was used to obtain a subsample (typically 0.2–0.5 g) for analysis. The core did not contain large plant or shell fragments suitable for radiocarbon dating; instead, plant fragments, seeds, and bulk sediment samples were collected for radiocarbon dating. One sample was collected from just below the sand layer; three more samples were collected from marsh sediments between the sand layer and base of the core. Radiocarbon ages were calibrated using the Calib Radiocarbon Calibration Program and intcal13.14c calibration dataset (Reimer *et al.*, 2016).

The elevation profile function in Google Earth was used to construct a topographic profile from the marsh, across the wooded dune barrier, to the beach and tidal flats bordering the Gulf of Tonkin (Google Earth, 2018) (Figure 2). The profile was located in an area that appeared undisturbed by anthropogenic activities (farther south, the dunes had been disturbed by recent excavations; see Figure 2). The lowest tide level along this profile on Google Earth images from previous years is about 0.3 m (image from 19 May 2015), suggesting that datum for the Google Earth profile (0 m in Figure 2) probably closely coincides with the Vietnamese National Datum (lowest annual tide level at Hon Dau Island; Boyd and Lam, 2004). The boundary between the dry, bright, white beach and the wet, grey tidal flats, visible on Figure 2, is assumed to approximately represent the landward limit of the intertidal zone (covered by "normal" tides). This boundary is at an elevation of 3.2 m on the Google Earth profile; the midpoint of the intertidal range is 1.6 m, which is assumed to approximate mean sea level.

While conducting reconnaissance along the planned profile line, a layer of weakly cemented beachrock was discovered between the beach and the wooded dunes (Figure 3). The base

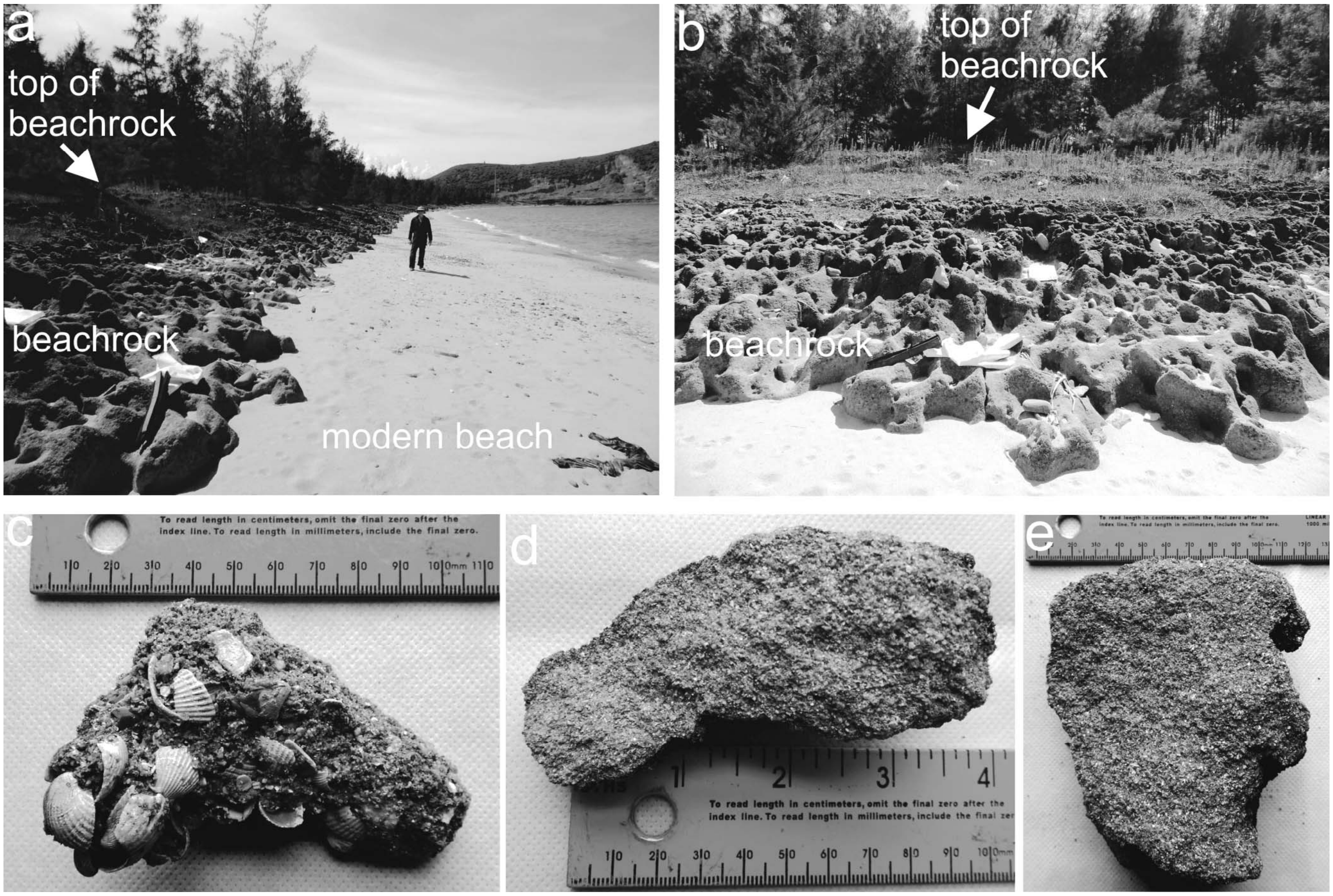

Figure 3. (a) View north along the beach, near the line of the elevation profile. The beachrock lies between the modern beach and the wooded dunes. The highest exposure of beachrock is ~2.5 m above the beach. (b) View west showing the heavily pitted beachrock where large rounded cobbles have been weathered out of the rock. (c) Sample of lower beachrock showing gravel- and coarse-sand-sized clasts and whole shells. (d) Sample of mid beachrock (about 1.25 m above the beach) showing coarse sand and abundant coarse shell fragments. (e) Sample of upper beachrock (about 2.5 m above the beach) showing finer sand and finer shell fragments. Ruler has mm and inch divisions.

of the beachrock coincides with the top of the modern beach; the top of the beachrock is estimated to be 2.5 m higher within the wooded dunes, where small outcroppings of beachrock emerge from the dune sand. The estimated elevations of the intertidal flats, modern beach, beachrock, and wooded dunes have been added to the elevation profile in Figure 2.

No plant remains could be found in the beachrock, so small shells were collected from the lower part of the beachrock for radiocarbon dating. Reworking of shells is a common problem that affects the accuracy of radiocarbon age determinations of littoral deposits. To improve the chances of obtaining an accurate age of the beachrock, three whole shells were collected for radiocarbon dating from the same small piece of beachrock (Figure 3c). Whole, small, unabraded shells were selected on the assumption that these delicate shells would not survive substantial reworking and would more closely date the time of deposition of the beachrock sediments. Radiocarbon ages were calibrated using the Calib Radiocarbon Calibration Program and marine13.14c calibration dataset (Reimer *et al.*, 2016).

RESULTS

The sand layer in the subsurface of the marsh at core site V3 meets many of the criteria for a washover sand layer deposited by a typhoon storm surge. Visually, the sand forms a distinct layer that is sandier and lighter in color than the enclosing muddy marsh deposits. The sand layer contains abundant well-rounded small shell fragments that are not visible in any other part of the 0.9-m-long core. The basal contact of the layer is very sharp and is marked by an abrupt drop in sand content, from 60% at the base of the sand layer to 21% in the immediately underlying marsh deposit. Moisture content and organic content are lower in the sand layer than in any other part of the core. Carbonate content reaches a peak within the sand layer, probably reflecting the abundant shell content. Sand content throughout the layer is higher than in any other part of the core, with the exception of a single sample at 65-cm depth, which could be the result of downward bioturbation of sand by burrowing organisms (Figure 4).

Assuming that the thin sand layer found in gouge core 6 is part of the same washover deposit found in core V3 suggests an

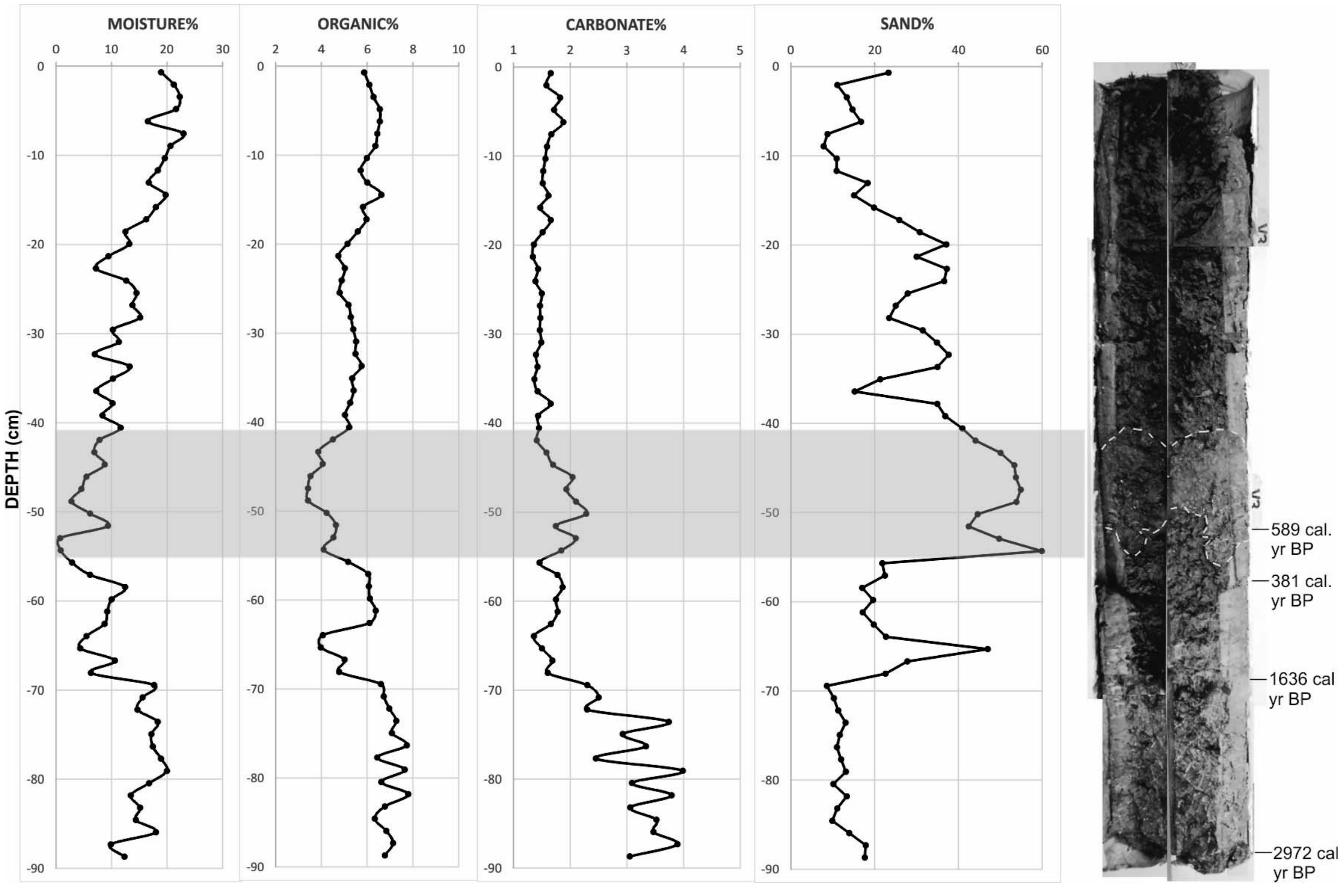

Figure 4. Results of analyses of core V3. Depths are uncompacted depths. Approximate locations and ages of radiocarbon-dated samples are shown (ages are midpoints of 2σ calibrated age ranges). White dashed lines approximate upper and lower contacts of sand layer.

extensive sand sheet extending over at least 150 m of the former marsh surface. The occurrence of this sand layer at only two of nine core sites indicates that the washover deposit is not continuous, but rather that it has a "patchy" distribution, similar to the distribution of washover sand deposited by Hurricane Rita in a Louisiana coastal marsh, as reported by Williams (2013). Reasons for this uneven distribution of the washover deposit could possibly include the following: the sand preferentially filled in low spots on the marsh surface; lobes of washover sand covered some parts of the marsh surface but not others; or thinner washover deposits, in some cases, have been rendered unrecognizable by bioturbation. The abundant shell fragments in the sand layer and the presence of the sand layer in cores nearer the coast, but not in the five cores farthest from the coast, argues against a fluvial source and for a marine source of the sand.

All samples from core V3 were examined for foraminiferal microfossils, but none were found in any of the samples. This is not uncommon in sandy washover deposits because delicate foraminiferal tests can be destroyed by abrasion and dissolution (Haslett, Bryant, and Curr, 2000; Horton, Rossi, and Hawkes, 2009; Murray, 1973). The samples collected for radiocarbon dating returned radiocarbon ages of 575 ± 27, 310 ± 27, 1729 ± 39, and 2858 ± 28 YBP from uncompacted depths of 52 cm, 57 cm, 69 cm, and 88 cm, respectively (Figure 4; Table 1).

Characteristics of the beachrock vary with elevation and closely match characteristics of the modern beach and tidal flat. The lower beachrock contains rounded pebbles, gravel-sized clasts and coarse sand, and whole and fragmented shells (Figure 3c). All of these features can be found in the modern tidal flat. The middle part of the beachrock has well-sorted coarse sand and coarse shell fragments and is similar in character to the lower part of the modern beach (Figure 3d). The upper beachrock contains well-sorted finer sand and shell

Table 1. *Radiocarbon dating results.*

Sample ID	Description	Radiocarbon age YBP	Calibrated age YBP 2σ limits
BR1	Beach rock shell	4858 ± 47	5003–5304
BR2	Beach rock shell	3887 ± 31	3733–3980
BR3	Beach rock shell	3524 ± 42	3318–3550
V3-52	Core sample	575 ± 27	532–645
V3-57	Core sample	310 ± 27	302–460
V3-69	Core sample	1729 ± 39	1549–1722
V3-88	Core sample	2858 ± 28	2880–3063

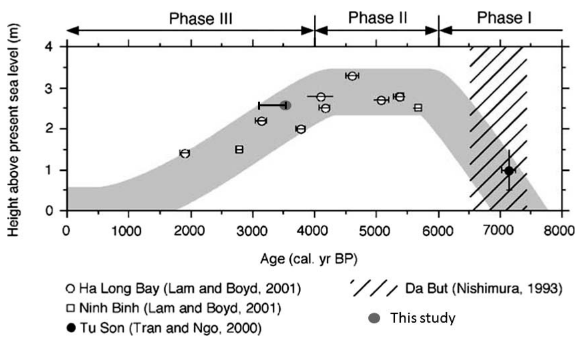

Figure 5. Sea-level curve in the Song Hong delta region during the past 8000 years (modified from Tanabe [2003]).

fragments, matching the character of the upper modern beach (Figure 3e). The shells taken from the lower beachrock returned radiocarbon ages of 4858 ± 47, 3887 ± 31, and 3524 ± 42 YBP (Table 1).

DISCUSSION

The variation in ages of the three shells collected from the beachrock suggests that the two older shells are probably reworked. The beachrock cannot be older than the maximum age of the youngest shell (3550 cal. YBP), and this age is tentatively assigned to the beachrock. The beachrock resembles the modern beach and tidal flat and is interpreted as a beach deposit that formed approximately 3550 cal. YBP during the previously documented sea-level highstand. Following the fall of sea level in the late Holocene, the beach deposit became supratidal and weakly cemented, probably by carbonates in sea spray (Kelletat, 2006). The lower beachrock is clearly undergoing erosion and is almost certainly truncated. The upper beachrock is more sheltered from weathering and erosion because it is above the reach of normal tides and waves. Because the upper beachrock closely resembles the upper modern beach and is elevated 2.5 m above it, it represents a 2.5-m-higher sea level no older than 3550 cal. YBP.

A mid-Holocene highstand, representing the culmination of the Post-Glacial Marine Transgression, is widely documented in Southeast Asia, including the Thai–Malay Peninsula (Horton *et al.*, 2005; Tjia, 1996), Gulf of Thailand (Choowong, 2002; Choowong *et al.*, 2004; Sinsakul, 1990, 1992; Somboon and Thiramongkol, 1992), Andaman Sea (Scheffers *et al.*, 2012), Singapore (Bird *et al.*, 2007, 2010; Hesp *et al.*, 1998), and the Straits of Malacca (Geyh, Kudrass, and Streif, 1979; Streif, 1979). In southern Vietnam, beachrock outcrops have been used to reconstruct Holocene sea-level changes (Stattegger *et al.*, 2013). These studies found evidence of rapid sea-level rise in the early Holocene, culminating in the mid-Holocene highstand, followed by the gradual fall of the sea to its present level. The studies also reveal considerable spatial variability in the magnitude of the highstand, from 1.5 to 5 m, probably reflecting hydroisostatic effects (Horton *et al.*, 2005).

In Northern Vietnam, studies of archaeological sites at Da But (Nishimura, 1993), marine notches at Ha Long Bay and Ninh Binh (Lam and Boyd, 2001), and marine terraces on the Song Hong delta (Tran and Ngo, 2000), suggest that the sea reached its present level 8000–7000 cal. YBP, continued to rise and stabilized at a highstand of 2–3 m between 6000 and 4000 cal. YBP, and then fell to its present level from 4000 to 0 cal. YBP. Given the apparent paleoelevation of sea level recorded by the beachrock (2.5 m) and the beachrock's maximum age of 3550 cal. YBP, the dated beachrock probably formed between about 3100 and 3550 cal. YBP, when sea level in the study area was 2.5 m higher than today (Figure 5).

It is tempting to conclude that the apparent washover deposit in core V3 was formed by typhoon overwash during the mid-Holocene sea-level highstand when the relative height of the coastal barrier may have been 2.5 m lower than today; however, the radiocarbon ages from core V3 do not support this interpretation. The dated sample collected from 52-cm depth immediately below the sand layer suggests that its age is around 589 cal. YBP. The reliability of the radiocarbon dates is uncertain; it may be that the dated materials from the core were contaminated by roots or bioturbated by burrowing organisms; for example, the dates of 589 cal. YBP and 381 cal. YBP are clearly "inverted" (older age above younger age) (Figure 4). However, it seems unlikely that all four dates are erroneously "young," and the sand layer is most likely late Holocene in age.

The relatively young age of the sand layer suggests that typhoon overwash may have occurred in the late Holocene, perhaps around 589 cal. YBP, and emplaced the sand layer in the marsh. Sea level would have been close to its present level at this time (Figure 5), and if the coastal barrier was at the same height as today, this would imply an exceptionally large storm surge capable of transporting littoral sands over a ~6.4 m barrier. The dimensions of the coastal barrier in past centuries and millennia are unknown. Although the beachrock was presumably in place by ~3100 cal. YBP at the latest, the wooded dunes may have formed after emplacement of the washover sand layer. If this was the case, the coastal barrier may have been ~2 m lower when overwash occurred, and a correspondingly smaller storm surge could have transported the sand over the barrier and into the marsh (Figure 2).

Another possibility is that the sand layer in the marsh was deposited by a tsunami wave that overtopped the coastal barrier. There are historical accounts of tsunami waves striking the coast of Vietnam (Vu and Nguyen, 2008). An account from the late 19^{th}/early 20^{th} century describes a wave more than 3 m in height overwashing the coast in Dien Chau District, a few kilometers north of the study area. The wave occurred on a calm day and caused inundation of greater than 1.5 m depth, extending over 1 km inland. In the absence of known earthquakes in the region during that time period, a nearby submarine landslide has been suggested as the possible source of the tsunami (Nguyen *et al.*, 2007). It is unlikely that the sand layer uncovered in the marsh records this very recent tsunami, but it may have resulted from an earlier tsunami in the same region.

CONCLUSIONS

Beachrock found in the study area records a beach that formed between ~3100 and 3550 cal. YBP and indicates a 2.5-

m-higher sea-level at that time. This finding is in good agreement with other studies of a mid-Holocene sea-level highstand in Northern Vietnam. The relatively thick sand and shell layer found in the subsurface of the freshwater marsh is tentatively identified as a washover deposit. The sandy texture of the deposit and abundant shell content suggest that the adjacent tidal flats, beach, and dunes were likely sources of sediment. The sharp basal contact of the sand layer suggests it resulted from an abrupt, short-lived depositional event that deposited an anomalous sand layer over a distance of at least 150 m on the marsh surface. The occurrence of the sand layer in cores nearer the coast, but not in cores farther inland, and the shell content rule out a fluvial flood origin. The age of the washover deposit is uncertain; radiocarbon-dated material immediately below the sand layer suggests it is about 589 cal. YBP, but the presence of inverted dates in the core suggests some uncertainty in ages, most likely resulting from contamination by roots or sediment displacement caused by bioturbation. Based on the four radiocarbon dates obtained from the core, the sand layer is most likely late Holocene in age and was emplaced when sea level was at, or close to, its present position. Overwash could have been accomplished by an exceptionally large storm surge that overtopped the coastal barrier in the late Holocene when barrier height was presumably similar to its height today. An alternative explanation is that the washover deposit resulted from a tsunami wave that overtopped the coastal barrier. There are historical accounts of tsunami waves in the vicinity of the study area, possibly caused by nearby submarine landslides. If the core records about 3000 years of sedimentation, the lack of other recognizable washover deposits in the core suggests that overwash of a magnitude that formed the sand layer is a rare event at this site. Given the lack of information on prehistoric washover deposits in Vietnam, further research at this site is warranted to better define the stratigraphy and age of the apparent washover deposit.

ACKNOWLEDGMENTS

This material is based upon work supported by the National Geographic Society/Waitt Grants program under Grant No. W473-16. The manuscript was improved by comments of two anonymous reviewers.

LITERATURE CITED

Bengtsson, L.; Hodges, K.I.; Esch, M.; Keenlyside, N.; Kornblueh, L.; Luo, J.-J., and Yamagata, T., 2007. How may tropical cyclones change in a warmer climate? *Tellus A*, 59(4), 539–561.

Bird, M.I.; Austin, W.E.N.; Wurster, C.M.; Fifield, L.K.; Mojtahid, M., and Sargeant, C., 2010. Punctuated eustatic sea-level rise in the early mid-Holocene. *Geology*, 38(9), 803–806.

Bird, M.I.; Fifield, L.K.; Teh, T.S.; Chang, C.H.; Shirlaw, N., and Lambeck, K., 2007. An inflection in the rate of early mid-Holocene eustatic sea-level rise: A new sea-level curve from Singapore. *Estuarine, Coastal and Shelf Science*, 71(3–4), 523–536.

Boyd, W.E. and Lam, D.D., 2004. Holocene elevated sea levels on the north coast of Vietnam. *Geographical Research*, 42(1), 77–88.

Camargo, S.J., 2013. Global and regional aspects of tropical cyclone activity in the CMIP5 models. *Journal of Climate*, 26, 9880–9902.

Chan, J.C.L., 1985. Tropical cyclone activity in the Northwest Pacific in relation to the El Niño/Southern Oscillation phenomenon. *Monthly Weather Review*, 113, 599–606.

Choowong, M., 2002. The geomorphology and assessment of indicators of sea-level changes to study coastal evolution from the Gulf of Thailand. *Proceedings of the International Symposium on Geology of Thailand* (Thailand, Department of Mineral Resources), pp. 207–220.

Choowong, M.; Ugai, H.; Charoentitirat, T.; Charusiri, P.; Daorerk, V.; Songmuang, R., and Ladachart, R., 2004. Holocene biostratigraphical records in coastal deposits from Sam Roi Yod National Park, Prachuap Khiri Khan, Western Thailand. *Natural History Journal of Chulalongkorn University*, 4(2), 1–18.

Christensen, J.H.; Kanikicharla, K.K.; Aldrian, E.; An, S.-I.; Cavalcanti, I.F.A.; de Castro, M.; Dong, W.; Goswami, P.; Hall, A.; Kanyanga, J.K.; Kitoh, A.; Kossin, J.; Lau, N.-C.; Renwick, J.; Stephenson, D.B.; Xie, S.-P., and Zhou, T., 2013. Climate phenomena and their relevance for future regional climate change. *In:* Intergovernmental Panel on Climate Change (ed.), *Climate Change 2013—The Physical Science Basis: Working Group I Contribution to the Fifth Assessment Report of the Intergovernmental Panel on Climate Change*. Cambridge, United Kingdom: Cambridge University Press, pp. 1217–1308.

Donnelly, J.P., 2005. Evidence of past intense tropical cyclones from backbarrier salt pond sediments: A case study from Isla de Culebrita, Puerto Rico, USA. *In:* Finkl, C.W. (ed.), *The Sun, Earth and Moon: A Tribute to Rhodes W. Fairbridge*. *Journal of Coastal Research*, Special Issue No. 42, pp. 201–210.

Donnelly, J.P.; Bryant, S.S.; Butler, J.; Dowling, J.; Fan, L.; Hausmann, N.; Newby, P.; Shuman, B.; Stern, J.; Westover, K., and Webb III, T., 2001a. 700 yr sedimentary record of intense hurricane landfalls in Southern New England. *Geological Society Bulletin*, 113(6), 714–727.

Donnelly, J.P.; Butler, J.; Roll, S.; Wengren, M., and Webb III, T., 2004. A backbarrier overwash record of intense storms from Brigantine, New Jersey. *Marine Geology*, 210(1–4), 107–121.

Donnelly, J.P.; Roll, S.; Wengren, M.; Butler, J.; Lederer, R., and Webb III, T., 2001b. Sedimentary evidence of intense hurricane strikes from New Jersey. *Geology*, 29(7), 615–618.

Donnelly, J.P. and Woodruff, J.D., 2007. Intense hurricane activity over the past 5,000 years controlled by El Niño and the West African monsoon. *Nature*, 447, 465–468.

Elsner, J.B. and Liu, K.-b., 2003. Examining the ENSO-typhoon hypothesis. *Climate Research* 25, 43–54.

Emanuel, K.A., 2013. Downscaling CMIP5 climate models shows increased tropical cyclone activity over the 21st century. *Proceedings of the National Academy of Sciences of the United States of America*, 110(3), 12219–12224. doi/10.1073/pnas.1301293110

Emanuel, K.A. and Nolan, D.S., 2004. Tropical cyclone activity and global climate. *Bulletin of the American Meteorological Society*, 85, 666–667.

Fan, D. and Liu, K.-b., 2008. Perspectives on the linkage between typhoon activity and global warming from recent research advances in paleotempestology. *Chinese Science Bulletin,* 53(19), 2907–2922.

Frappier, A.; Knutson, T.; Liu, K.-b., and Emanuel, K., 2007. Perspective: Coordinating paleoclimate research on tropical cyclones with hurricane-climate theory and modelling. *Tellus A*, 59(4), 529–537. doi:10.1111/j.1600-0870.2007.00250.x

García-Herrera, R.; Gimeno, L.; Ribera, P., and Hernández, E., 2005. New records of Atlantic hurricanes from Spanish documentary sources. *Journal of Geophysical Research*, 110(D03109), 1–7.

García-Herrera, R.; Gimeno, L.; Ribera, P.; Hernández, E.; González, E., and Fernández, G., 2007. Identification of Caribbean basin hurricanes from Spanish documentary sources. *Climate Change*, 83(1–2), 55–85. doi:10.1007/s10584-006-9124-4

García-Herrera, R.; Rubio Durán, F.; Wheleer, D.; Hernández, E.; Prieto, M.R., and Gimero, L., 2004. The use of Spanish and British documentary sources in the investigation of Atlantic hurricane incidence in historical times. *In:* Murnane, R.J. and Liu, K-b. (eds.), *Hurricanes and Typhoons: Past, Present, and Future*. New York: Columbia University Press, pp. 149–176.

Garmin, 2007. *Garmin Etrek HC Owners Manual*. Olathe, Kansas: Garmin, 32p.

Geyh, M.A.; Streif, H., and Kudrass, H.-R., 1979. Sea-level changes during the late Pleistocene and Holocene in the Strait of Malacca. *Nature*, 278, 441–443.

Google Earth, 2018. *Cam River Mouth, Vietnam*. https://www.google.com/earth/

Grossman, M. and Zaiki, M., 2009. Reconstructing typhoons in Japan in the 1880s from documentary records. *Weather*, 64(12), 315–322.

Gualdi, S.; Scoccimarro, E., and Navarra, A., 2008. Changes in tropical cyclone activity due to global warming: Results from a high-resolution coupled general circulation model. *Journal of Climate*, 21, 5204–5228.

Haslett, S.K.; Bryant, E.A., and Curr, R.H.F., 2000. Tracing beach sand provenance and transport using Foraminifera: Preliminary examples from Northwest Europe and Southeast Australia. *In:* Foster, D.L. (ed.), *Tracers in Geomorphology*. Chichester, U.K.: Wiley, pp. 437–452.

Heiri, O.; Lotter, A.F., and Lemcke, G., 2001. Loss on ignition as a method for estimating organic and carbonate content in sediments: Reproducibility and comparability of results. *Journal of Paleolimnology*, 25(1), 101–110.

Hesp, P.A.; Hung, C.C.; Hilton, M.; Ming, C.L., and Turner, I.M., 1998. A first tentative Holocene sea-level curve for Singapore. *Journal of Coastal Research*, 14(1), 308–314.

Hodge, J. and Williams, H.F.L., 2016. Deriving spatial and temporal patterns of coastal marsh aggradation from hurricane storm surge marker beds. *Geomorphology*, 274, 50–63.

Horton, B.P.; Gibbard, P.L.; Milne, G.M.; Morley, R.J.; Purin Tavaragul, C., and Stargardt, J.M., 2005. Holocene sea levels and palaeoenvironments, Malay–Thai Peninsula, Southeast Asia. *The Holocene* 15, 1199–1213.

Horton, B.P.; Rossi, V., and Hawkes, A.D., 2009. The sedimentary record of the 2005 hurricane season from the Mississippi and Alabama coastlines. *Quaternary International*, 195(1–2), 15–30.

Kelletat, D., 2006. Beachrock as sea-level indicator? Remarks from a geomorphological point of view. *Journal of Coastal Research*, 22(6), 1558–1564.

Knutson, T.R.; McBride, J.L.; Chan, J.; Emanuel, K.; Holland, G.; Landsea, C.; Held, I.; Kossin, J.P.; Srivastava, A.K., and Sugi, M., 2010. Tropical cyclones and climate change. *Nature Geoscience*, 3, 157–163.

Lam, D.D. and Boyd, W.E., 2001. Some facts of sea-level fluctuation during the late Pleistocene–Holocene in Ha Long Bay and Ninh Binh area. *Journal of Sciences of the Earth*, 23, 86–91.

Lane, P.; Donnelly, J.P.; Woodruff, J.D., and Hawkes, A.D., 2011. A decadally-resolved paleohurricane record archived in the late Holocene sediments of a Florida sinkhole. *Marine Geology*, 287(1–4), 14–30.

Liu, K.-b. and Fearn, M.L., 1993. Lake-sediment record of late Holocene hurricane activities from coastal Alabama. *Geology*, 21(9), 793–796.

Liu, K.-b. and Fearn, M.L., 2000a. Reconstruction of prehistoric landfall frequencies of catastrophic hurricanes in northwestern Florida from lake sediment records. *Quaternary Research*, 54(2), 238–245.

Liu, K.-b. and Fearn, M.L., 2000b. Holocene history of catastrophic hurricane landfalls along the Gulf of Mexico coast reconstructed from coastal lake and marsh sediments. *In:* Ning, Z.H. and Abdollahi, K.K. (eds.), *Current Stresses and Potential Vulnerabilities: Implications of Global Change for the Gulf Coast Region of the United States*. Baton Rouge, Louisiana: Franklin, pp. 38–47.

Liu, K.B.; Shen, C., and Louie, K.S., 2001. A 1000-year history of typhoon landfalls in Guangdong, southern China, reconstructed from Chinese historical documentary records. *Annals of the Association of American Geographers,* 91(3), 453–464.

McCloskey, T.A.; Bianchette, T.A., and Liu, K.B., 2013. Track patterns of landfalling and coastal tropical cyclones in the Atlantic Basin, their relationship with the North Atlantic Oscillation (NAO), and the potential effect of global warming. *American Journal of Climate Change*, 2(3A), 12–22.

McCloskey, T.A. and Keller, G., 2009. 5000 year sedimentary record of hurricane strikes on the central coast of Belize. *Quaternary International*, 195(1–2), 53–68.

Mock, C.J., 2004. Tropical cyclone reconstructions from documentary records; Examples from South Carolina. *In:* Murnane, R.J. and Liu, K-b. (eds.), *Hurricanes and Typhoons: Past, Present, and Future*. New York: Columbia University Press, pp. 121–148.

Murakami, H.; Mizuta, R., and Shindo, E., 2012. Future changes in tropical cyclone activity projected by multi-physics and multi-SST ensemble experiments using the 60-km-mesh MRI-AGCM. *Climate Dynamics*, 39(9–10), 2569–2584.

Murakami, H.; Wang, B., and Kitoh, A., 2011. Future change of western North Pacific typhoons: projections by a 20-km-mesh global atmospheric model. *Journal of Climate*, 24, 1154–1169.

Murakami, H.; Wang, Y.; Yoshimura, H.; Mizuta, R.; Sugi, M.; Shindo, E.; Adachi, Y.; Yukimoto, S.; Hosaka, M.; Kusunoki, S.; Ose, T., and Kitoh, A., 2012. Future changes in tropical cyclone activity projected by the new high-resolution MRI-AGCM. *Journal of Climate*, 25, 3237–3260.

Murray, J.W., 1973. *Distribution and Ecology of Living Benthic Foraminiferids*. London: Heinemann, 274p.

Nott, J. and Hayne, M., 2001. High frequency of 'super-cyclones' along the Great Barrier Reef over the past 5,000 years. *Nature*, 413(6855), 508–512.

Nguyen, D.T., 1991. Marine terraces of Indochina. *Mineral Resources Development Series,* 60. New York: United Nations, pp. 47–50.

Nguyen, V.L.; Duong, Q.H.; Bui, T.X., and Nguyen, B.D., 2007. *Characteristics and properties of earthquake in South China Sea and surrounding areas*. Report submitted to IMHEN, 41p.

Nishimura, M., 1993. Shell midden sites in Vietnam and Thailand. *Journal of Southeast Asian Archaeology*, 13, 25–50.

Pielke, Jr., R.A.; Landsea, C.; Mayfield, M.; Laver, J., and Pasch, R., 2005. Hurricanes and global warming. *Bulletin of the American Meteorological Society,* 86, 1571–1575.

Pirazzoli, P.A., 1991. *World Atlas of Holocene Sea-Level Changes*. Amsterdam: Elsevier, 300p.

Reimer, P.J.; Bard, E.; Bayliss, A.; Beck, J.W.; Blackwell, P.G.; Bronk Ramsey, C.; Buck, C.E.; Cheng, H.; Edwards, R.L.; Friedrich, M.; Grootes, P.M.; Guilderson, T.P.; Haflidason, H.; Hajdas, I.; Hatté, C.; Heaton, T.J.; Hogg, A.G.; Hughen, K.A.; Kaiser, K.F.; Kromer, B.; Manning, S.W.; Niu, M.; Reimer, R.W.; Richards, D.A.; Scott, E.M.; Southon, J.R.; Turney, C.S.M., and van der Plicht, J., 2016. IntCal13 and MARINE13 radiocarbon age calibration curves 0–50,000 years cal BP. *Radiocarbon*, 55(4), 11869–1887. doi:10.2458/azu_js_rc.55.16947

Scheffers, A.; Brill, D.; Scheffers, S.; Kelletat, D., and Fox, K., 2012. Holocene sea levels along the Andaman Sea coast of Thailand. *The Holocene*, 22(10), 1169–1180.

Sinsakul, S., 1990. Evidence of sea level changes in the coastal areas of Thailand: a review. *Workshop on Global Environmental Change, Chiang Mai, Thailand*. Economic and Social Commission for Asia and the Pacific-Coordination of Joint Prospecting of Mineral Resources in Offshore Areas of Asia (ESCAP-CCOP).

Sinsakul, S., 1992. Evidence of quaternary sea level changes in the coastal areas of Thailand: a review. *Journal of Southeast Asian Earth Science*, 7(1), 23–37.

Somboon, J.R.P. and Thiramongkol, N., 1992. Holocene highstand shoreline of the Chao Phyraya delta, Thailand. *Journal of Southeast Asian Earth Science,* 7(1), 53–60.

Streif, H., 1979. Holocene sea-level changes in the Straits of Malacca. *Proceedings of the 1978 International Symposium on Coastal Evolution in the Quaternary* (Sao Paolo: IGCP Project 61), pp. 552–572.

Stattegger, K.; Tjallingii, R.; Saito, Y.; Michelli, M.; Thanh, N.T., and Wetzel, A., 2013. Mid to late Holocene sea-level reconstruction of southeast Vietnam using beachrock and beachridge deposits. *Global and Planetary Change*, 110(B), 214–222.

Stowasser, M.; Wang, Y., and Hamilton, K., 2007. Tropical cyclone changes in the Western North Pacific in a global warming scenario. *Journal of Climate*, 20, 2378–2396.

Sugi, M.; Yoshida, K., and Murakami, H., 2015. More tropical cyclones in a cooler climate? *Geophysical Research Letters,* 42(16), 6780–6784.

Switzer, A.D.; Gouramanis, C.; Dura, T.; Lam, D.D.; Hoang, L.V.; Sloss, C.R.; Hoang, Q.D.; Lee, Y.S.; Chan, M.M., and Pham, D.T.,

2011. Geological and geomorphological impacts of two large typhoons from the central coast of Vietnam. *Proceedings of the American Geophysical Union, Fall Meeting 2011* (San Francisco, California), abstract id OS33A-1633.

Tanabe, S., 2003. Song Hong (Red River) delta evolution related to millennium-scale Holocene sea-level changes. *Quaternary Science Reviews*, 22(21–22), 2345–2361.

Tanabe, S.; Saito, Y.; Lan, V.; Hanebuth, T.; Lan, N., and Kitamura, A., 2006. Holocene evolution of the Song Hong (Red River) delta system, Northern Vietnam. *Sedimentary Geology*, 187(1–2), 29–61.

Tjia, H.D., 1996. Sea-level changes in the tectonically stable Malay–Thai Peninsula. *Quaternary International*, 31, 95–101.

Tory, J.; Chand, S.S.; McBride, J.L.; Ye, H., and Dare, R.A., 2013. Projected changes in late-twenty-first-century tropical cyclone frequency in 13 coupled climate models from phase 5 of the Coupled Model Intercomparison Project. *Journal of Climate*, 26, 9946–9959.

Tran, N. and Ngo, Q.T., 2000. Development history of deposits in the Quaternary of Vietnam. *In:* Nguyen, T.V. (ed.), *The Weathering Crust and Quaternary Sediments in Vietnam*. Hanoi: Department of Geology and Minerals of Vietnam, pp. 177–192.

Vu, C. and Nguyen, D.X., 2008. Tsunami risk along Vietnamese coast. *Journal of Water Resources and Environmental Engineering*, 23, 24–32.

Walsh, K.J.E.; Camargo, S.J.; Vecchi, G.A.; Daloz, A.S.; Elsner, J.; Emanuel, K.; Horn, M.; Lim, Y.-K.; Roberts, M.; Patricola, C.; Scoccimarro, E.; Sobel, A.H.; Strazzo, S.; Villarini, G.; Wehner, M.; Zhao, M.; Kossin, J.; LaRow, T.; Oouchi, K.; Schubert, S.; Wang, H.; Bacmeister, J.; Chang, P.; Chauvin, F.; Jablonowski, C.; Murakami, H.; Ose, T.; Reed, K.A.; Saravanan, R.; Yamada, Y.; Zarzycki, C.M.; Vidale, P.-L.; Jonas, J.A., and Henderson, N., 2014. Hurricanes and climate: the U.S. CLIVAR working group on hurricanes. *Bulletin of the American Meteorological Society*. doi:10.1175/BAMS-D-13-00242.1

Walsh, K.J.E., 2014. *8th International Workshop on Tropical Cyclones*. Topic 5.1 Interaction with climate change. December 1–10, 2014, Jeju, Republic of Korea. http://www.iwtc8.org/documents/Topic5.1_InteractionwithClimateChange.pdf

Webster, P.J.; Holland, G.J.; Curry, J.A., and Chang, H.R., 2005. Changes in tropical cyclone number, duration, and intensity in a warming environment. *Science*, 309(5742), 1844–1846.

Williams, H.F.L., 2013. 600-year sedimentary archive of hurricane strikes in a prograding beach ridge plain, southwestern Louisiana. *Marine Geology*, 336, 170–183.

Williams, H.; Choowong, M.; Phantuwongraj, S.; Surakietchai, P.; Thongkhao, T.; Kongsen, S., and Simon, E., 2016. Geologic records of Holocene typhoon strikes on the Gulf of Thailand coast. *Marine Geology*, 372, 66–78.

Woodruff, J.D.; Donnelly, J.P., and Okusu, A., 2009. Exploring typhoon variability over the mid to- late Holocene: evidence of extreme coastal flooding from Kamikoshiki, Japan. *Quaternary Science Reviews*, 28(17–18), 1774–1785.

Ying, M.; Knutson, T.R.; Kamahori, H., and Lee, T-C., 2012. Impacts of climate change on tropical cyclones in the western North Pacific Basin. Part II: late twenty-first century projections. *Tropical Cyclone Research and Review*, 1(2), 231–241.

Yu, K.f.; Zhao, J.x.; Shi, Q., and Meng, Q.S., 2009. Reconstruction of storm/tsunami records over the last 4000 years using transported coral blocks and lagoon sediments in the southern South China Sea. *Quaternary International,* 195(1–2), 128–137.